0026-895X/02/6104-913–920$7.00
MOLECULAR PHARMACOLOGY
Copyright © 2002 The American Society for Pharmacology and Experimental Therapeutics
Mol Pharmacol 61:913–920, 2002

Vol. 61, No. 4
1361/974121
Printed in U.S.A.

Determinants of 4-Aminopyridine Sensitivity in a Human Brain Kv1.4 K^+ Channel: Phenylalanine Substitutions in Leucine Heptad Repeat Region Stabilize Channel Closed State

SUSAN I. V. JUDGE, JAY Z. YEH, JAMES E. GOOLSBY, MERVYN J. MONTEIRO, and CHRISTOPHER T. BEVER, JR.

Research and Neurology Services, VA Maryland Health Care System, Baltimore, Maryland (S.I.V.J., C.T.B.); Department of Neurology, University of Maryland School of Medicine, Baltimore, Maryland (S.I.V.J., C.T.B., M.J.M., J.E G.); Medical Biotechnology Center, University of Maryland Biotechnology Institute, Baltimore, Maryland (M.J.M.); and Department of Molecular Pharmacology and Biological Chemistry, Northwestern University Medical School, Chicago, Illinois (J.Z.Y.)

Received September 14, 2001; accepted January 15, 2002

This article is available online at http://molpharm.aspetjournals.org

ABSTRACT

The biophysical and pharmacological effects of individual phenylalanine-for-leucine (Phe-for-Leu) substitutions in the leucine heptad repeat region located at the cytosolic surface of the channel pore, on whole-cell K^+ currents, were studied in cloned and mutated human brain Kvl.4 K^+ channels (hKvl.4) transiently transfected into HeLa cells. Although L2 and L5 are not considered part of the 4-aminopyridine (4-AP) binding site, unlike the L4 heptad leucine, Phe substitutions at L2 (L464) or L5 (L485) increase 4-AP sensitivity by 400-fold, as seen previously in the L4F mutant channel (Judge et al., 1999). Greater depolarizing shifts manifest in the voltage dependence of activation and inactivation in L2F (20 mV) and L5F (30 mV) than in L4F (10 mV) relative to hKv1.4. L1F (L457) and L3F (L471) increase 4-AP sensitivity by 8- and 150-fold, respectively, and produce depolarizing shifts in activation of ~5 mV without affecting inactivation. The apparent free energy differences of 4-AP binding in each mutant suggest enhanced drug-channel interactions (L2F $\geq$ L4F $\geq$ L5F $>$ L3F $>$ L1F). Deactivation kinetics are accelerated in L2F (11-fold), L5F (8-fold), L1F (5-fold), and L3F (2-fold), at −50 mV. All Phe-for-heptad-Leu substitutions produce gating changes suggesting variable stabilization of the channel closed state conformation, with L1F, L2F, and L5F exhibiting the strongest correlations between altered gating and increased 4-AP sensitivity. If 4-AP blocks the open channel by promoting closure of the activation gate (recent Armstrong-Loboda model), then changes in the leucine heptad repeat that stabilize the channel closed state may contribute to increased 4-AP sensitivity by amplifying the mechanism of 4-AP block.

The leucine heptad repeat region, which is a highly conserved feature in K^+ channels spanning the S4−S5 linker and adjacent ends of the S4 and S5 segments at the cytosolic mouth of the ion translocation pore, plays a significant role in modulating the stability of channel open and closed state conformations. McCormack et al. (1989), the first to identify this sequence of regular leucine repeats (a pattern commonly referred to as a leucine-zipper in other proteins in which subunit interaction involves the formation of parallel coiled-coils) as a prevalent motif in voltage-gated K^+ channels, recognized the significance of its relationship to the S4 segment (voltage sensor). They correctly postulated involvement of the leucine heptad repeat region in the mechanism that couples movement of the S4 segment to the opening of the activation gate (Lopez et al., 1991; McCormack et al., 1991, 1994; Kirsch et al., 1993; Kirsch and Drewe, 1993; Aggarwal and MacKinnon, 1996; Shieh et al., 1997), which is formed by the S6 segments (Liu et al., 1997).

Site-directed mutagenesis studies in slowly inactivating, Kv2.1 and Kv3.1, delayed rectifier types of rat brain voltage-gated K^+ channels first demonstrated that critical molecular determinants of 4-aminopyridine (4-AP) sensitivity reside in the cytoplasmic halves of the S5 and S6 transmembrane segments (Kirsch et al., 1993; Shieh and Kirsch, 1994). Based on mutations that increased 4-AP sensitivity without affecting activation gating, they identified a trio of amino acids as signature determinants of 4-AP sensitivity and probable components of the 4-AP binding site: two in S6 and one in S5 that is the fourth leucine in the leucine heptad repeat region. More recent studies in a rapidly inactivating A-type human brain Kvl.4 K^+ channel (hKvl.4) confirmed that an analogous

This work was supported by separate Department of Veterans Affairs Merit Review Funding to S.I.V.J. and C.T.B. In addition, this work was supported by grant RG2127A2 from the National Multiple Sclerosis Society to C.T.B. and by grant AG11386 from the National Institutes of Health to M.J.M.

ABBREVIATIONS: 4-AP, 4-aminopyridine; hKv1.4, cloned human brain Kv1.4 potassium channel; *Sh*, *Shaker*; SS-inactivation, steady-state inactivation; LB, Luria broth; τ, time constant of inactivation; τ_{fast}, fast inactivation time constant; τ_{slow}, slow inactivation time constant; τ_{tails}, deactivation time constant; $V_{1/2}$, midpoint potential; ΔF, apparent free energy difference of binding; ρ, correlation coefficient.

L4F mutation enhanced block by 4-AP (Judge et al., 1999). However, the L4F mutation in hKv1.4 produced a larger increase of ~400-fold in block by 4-AP than the ~29-fold increase observed in Kv2.1 (Shieh and Kirsch, 1994). Although enhanced 4-AP sensitivity in hKv1.4 was shown to be independent of concurrent changes in inactivation gating kinetics, the L4F mutation in hKv1.4 (Judge et al., 1999), unlike in Kv2.1 (Shieh and Kirsch, 1994), was accompanied by changes in the kinetics and voltage dependence of current gating consistent with stabilization of the channel closed state.

Point mutations of individual heptad leucines to valine, in a *Drosophila melanogaster Shaker* (*Sh;* homologous to the vertebrate K^+ channel Kvl subfamily) A-type K^+ channel, suggest that opposing effects on both channel voltage dependence and 4-AP sensitivity depend on whether substitutions are located at the N- or C-terminal ends of the heptad repeat region (McCormack et al., 1991, 1994). Here, however, in hKvl.4, we show that individual Phe substitutions for the L1 (L1F), L2 (L2F), L3 (L3F), and L5 (L5F) heptad leucines, not considered 4-AP binding site components, all enhance 4-AP block with the extent of increased sensitivity corresponding to the magnitude of changes in activation and steady-state inactivation (SS-inactivation) voltage dependence, and in deactivation kinetics.

We show that individual Phe-for-heptad-leucine substitutions in hKv1.4 result in mutant channels that exhibit stronger stabilization of the closed state and greater affinity for 4-AP than the parent channel. These results are consistent with the current three-dimensional modeling of voltage-gated K^+ channels (H. R. Guy, personal communication) and recent models for the mechanism by which 4-AP blocks K^+ channels (Armstrong and Loboda, 2001; Loboda and Armstrong, 2001). Together, the patterns of these changes suggest that altered channel conformation alone may account for the increased 4-AP sensitivity in L1F, L2F, L4F, and L5F, whereas increased 4-AP sensitivity in L3F may also involve additional factors.

Materials and Methods

Cloning and Mutagenesis of hKvl.4. The human brain Kvl.4 cDNA was cloned and inserted into a pGEM eukaryotic expression vector as described previously (Janicki and Monteiro, 1997; Judge et al., 1999). Subsequently, a single amino acid substitution was made in the N-terminal end of the S6 transmembrane segment, located at the juncture between the S4−S5 linker and S5, to change the fourth heptad leucine (L4; residue 478) to phenylalanine (i.e., L4F; Judge et al., 1999). Additional individual point mutations were made in hKv1.4 to substitute Phe for each of the other heptad leucines at residues 457 (L1F), 464 (L2F), 471 (L3F), and 485 (L5F). Mutations were generated using the QuikChange Site-Directed Mutagenesis Kit (Stratagene, La Jolla, CA). Sets of two synthetic oligonucleotide primers containing single amino acid mutations for one of the four heptad leucines were generated at the University of Maryland Biopolymer Laboratory. The oligonucleotide primers, each complementary to the others and sharing 21 bases of homology on either side of the mutated leucine residue in cloned hKv1.4, were extended with *Pfu* DNA polymerase to generate mutant plasmids by polymerase chain reaction. The parental templates were digested away using *Dpn*I and the vector DNA incorporating the desired mutations was transformed into XL1-Blue Supercompetent Cells (Stratagene). The transformed XL1-Blue cells were plated on LB agar plates containing ampicillin (20 μg/ml) and single colonies picked for amplification in LB ampicillin broth (50 μg/ml). Sequencing was used to verify incorporation of the mutation into the vector. Plasmids were purified with QIAGEN Plasmid Mini Kit (QIAGEN, Valencia, CA) and submitted to the University of Maryland Biopolymer Laboratory for sequencing using primers generated to sites approximately 100 base pairs upstream of the mutation site. Colonies containing the mutated plasmid were amplified in 300 ml of ampicillin containing (50 μg/ml) LB broth and the plasmids were purified using QIAGEN Plasmid Maxi Kits.

Tissue Culture and DNA Transfection. The human epithelial-like HeLa cell line was grown in Dulbecco's modified Eagle's medium supplemented with 10% fetal bovine serum and glutamine and maintained in a 5% CO_2 incubator. Cells were trypsinized and cotransfected with either 20 μg each of the wild-type hKvl.4 or Leu-for-Phe mutated expression plasmids, and with 10 μg of the green fluorescent protein expression plasmid (pEGFP) plasmid DNAs (CLONTECH Laboratories, Inc., Palo Alto, CA) by electroporation using the Gene Pulser system (Bio-Rad, Hercules, CA). Cells were plated on 25 mm round glass cover slips (Fisher, Pittsburgh, PA), at a cell density of 1×10^4 cells/ml for whole-cell recording experiments beginning 48 h later.

Solutions, Reagents, and Toxins. A standard saline extracellular bath solution contained 145 mM NaCl, 5 mM KCl, 2 mM $CaCl_2$, 1 mM $MgCl_2$, 5.6 mM D-glucose, and 10 mM HEPES. The intracellular pipette solution contained 145 mM KCl, 4.5 mM NaCl, 0.1 mM $CaCl_2$, 1.2 mM $MgCl_2$, 1.1 mM EGTA, and 10 mM HEPES. Both the bath and pipette solutions were adjusted to pH 7.3 and osmolarities to between 290 and 330 mOsM. Just before recording, the solutions were passed through 0.2 μm Millipore (Bedford, MA) filters. Stock solutions of 4-AP (Sigma Chemical, St. Louis, MO) were prepared in the extracellular bath solution and stored at 4°C. The pEGFP plasmid DNA was transformed in DH1 bacterial cells, grown, aliquoted, and then stored at −20°C.

Patch Clamp Recording. Whole-cell currents were recorded from individual fluorescent HeLa cells visualized by a Nikon DIAPHOT-TMD inverted microscope (Tokyo, Japan) equipped with a TMD-EF epi-fluorescence attachment. An AXOPATCH 200B integrating patch clamp together with pClamp 6.0.3 software (Axon Instruments, Union City, CA) was used for data acquisition and analysis. Pipette offset adjustment, series resistance compensation, and pipette capacitance compensation were made electronically. Note that although maximal currents varied between 1 and 8 nA in cells transiently transfected with either wild-type or mutant channel cDNA, the degree of voltage-dependent shifts remained consistent for each channel type. Linear capacitance and leakage currents were subtracted on-line by a P/4 pulse protocol. Patch pipettes (3–5 MΩ) were fabricated from standard Kwik-Fil Borosilicate glass capillaries (World Precision Instruments, Sarasota, FL) using a Model P-97 Programable Brown-Flaming Micropipette Puller (Sutter, San Francisco, CA). Patch pipettes were not fire polished. All experiments were performed at room temperature (22−25°C).

Free Energy Difference of Binding. An apparent free energy difference (ΔF) is used here because the potency of 4-AP block in K^+ channels might be influenced by true binding and gating changes of the 4-AP bound channel. The apparent free energy difference in the five heptad leucine mutant channels were determined by the IC_{50} of 4-AP in each channel construct and calculated as $\Delta F = RT \ln(IC_{50}$ of mutant channel/IC_{50} of parent hKv1.4 channel), where R is 1.987 cal/mol and T (temperature) is 295°K (Pennington et al., 1996; Rauer et al., 1999).

Results

Compared with the parent hKv1.4 channel, the L1F, L2F, L3F, and L5F mutant channels, like L4F (Judge et al., 1999), produced current gating alterations consistent with stabilization of the channel closed state conformation. These indi-

vidual heptad leucine substitutions resulted in channels exhibiting variable slowing of the rate of current inactivation and speeding up of the rate of current deactivation. Parallel patterns of voltage dependent shifts, in the depolarizing direction, were observed for both current activation and steady-state inactivation in all mutant channels with the exception that L1F and L3F produced no voltage dependent effects on inactivation. Among these changes, the change in current deactivation is correlated best with the extent of increased 4-AP sensitivity seen in each channel construct. The properties of the new mutant channels will be compared with those of our previously characterized wild-type hKvl.4 and mutant L4F channels (Judge et al., 1999) throughout *Results*.

Channel Gating Effects of Phenylalanine for Heptad Leucine Substitutions in hKvl.4. Illustrated in Fig. l are typical families of whole-cell currents elicited from individual HeLa cells transiently transfected with L1F, L2F, L3F, or L5F cDNAs. All of the mutant channels exhibited a lengthening of the time constant of inactivation (τ). Shown are representative L2F (Fig. 1C) and L5F (Fig. 1F) currents that are fit by single exponentials like wild-type hKv1.4 (Fig. 1A). However, current inactivation kinetics in L2F (τ = 246.59 ms) and L5F (τ = 262.98 ms) more closely resemble the slow component of current decay in L4F (τ_{slow} = 209.97 ms), with approximately 10-fold slower rates of current inactivation than hKv1.4 (τ = 25.92 ms). As seen in the majority of L4F currents, current decay in the L1F (Fig. 1B) and L3F (Fig. 1D) currents is best fit by two exponentials. In the representative currents shown, τ_{fast} is slightly smaller in both L1F (τ_{fast} = 36.17 ms) and L3F (τ_{fast} = 34.11 ms) than in L4F (τ_{fast} = 50.41 ms), whereas τ_{slow} in L4F (τ_{slow} = 209.97 ms) lies intermediate between L1F (τ = 345.35 ms) and L3F (τ = 167.04 ms). The apparent speed (faster rates) of current inactivation (Fig. 1) has a qualitative rank ordering of L3F > L1F > hKv1.4 > L5F > L2F > L4F. This differs from the rank ordering of enhanced 4-AP block (Fig. 4) which is L2F > L5F > L4F > L3F > L1F > hKv1.4. To facilitate comparison of current inactivation between the wild-type and mutant channels, time intervals required for currents to decay to 50% and 90% of the peak current were also determined. The 90% decay times are 3.65 ms (hKv1.4), 5.51 ms (L1F), 29.15 ms (L2F), 5.46 ms (L3F), 11.85 ms (L4F), and 28.06 ms (L5F). The 50% decay times are 20.29 ms (hKv1.4), 28.90 ms (L1F), 341.20 ms (L2F), 25.61 ms (L3F), 98.38 ms (L4F), and 166.56 ms (L5F). A rank ordering of inactivation decay times is the same for determinations made at either 90 or 50% of the peak with hKv1.4 > L1F ≅ L3F > L4F > L5F > L2F. These inactivation decay times are not related to the rank order of 4-AP block, a result corroborating our previous conclusion that the inactivation gate is not a major determinant of 4-AP sensitivity in hKv1.4 (Judge et al., 1999).

As seen previously in L4F (Judge et al., 1999), Phe substitutions for each of the other heptad leucines resulted in an acceleration of current deactivation kinetics, as determined by exponential fit to the decay of tail currents. L2F and L5F exhibited 2- to 11-fold faster time constants of deactivation (τ_{tails}) than hKvl.4, which was comparable with L4F, whereas generally only 1- to 3-fold faster tail currents were seen in L1F and L3F (Table 1). Figure 2B shows representative tail current elicited from L5F at −60 and −100 mV. Although the current deactivation kinetics in L2F and L5F, like L4F, are not voltage-dependent, L1F and L3F retain the distinct voltage dependence seen in hKvl.4, at potentials positive to −70 mV (Fig. 2).

In hKvl.4, all Phe-for-Leu substitutions in the leucine heptad region produce shifts in the voltage dependence of current activation in the depolarizing direction. The mean midpoint potentials ($V_{1/2}$) of the conductance-voltage relationships are shifted approximately +5 mV in both L1F ($V_{1/2}$ = −9.71 ± 2.12 mV; n = 7) and L3F ($V_{1/2}$ = −9.48 ± 1.87 mV; n = 8), compared with hKvl.4 ($V_{1/2}$ = −12.76 ± 3.40 mV; n = 13). Greater depolarizing shifts were seen with the other mutant channels: a 10-mV shift in the L4F ($V_{1/2}$ = −4.73 ± 1.78 mV; n = 7), a 20-mV shift in L2F ($V_{1/2}$ = 12.43 ± 4.38

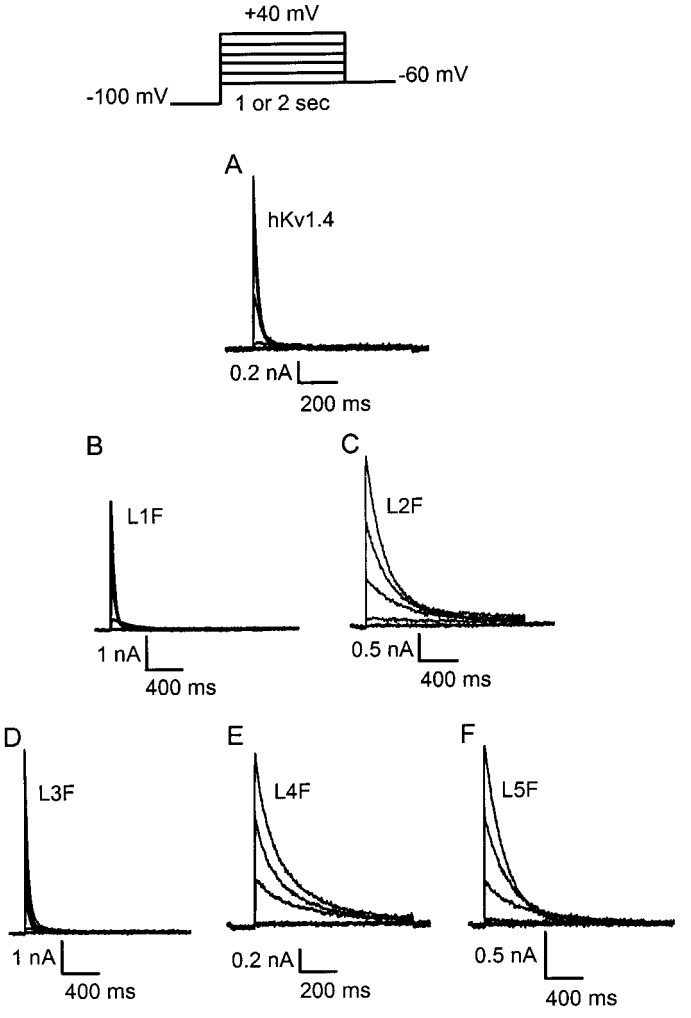

Fig. 1. Families of outward K^+ currents recorded from individual HeLa cells transfected with hKv1.4 or mutant K^+ channel DNAs. Shown are representative families of hKv1.4 (A), L1F (B), L2F (C), L3F (D), L4F (E), and L5F (F) K^+ currents. It can be seen that mutation of the L2, L4, and L5 heptad leucines to phenylalanine significantly slows the rate of current inactivation. Currents were elicited using the whole-cell P/4 subtraction pulse protocol shown above the current families. For hKv1.4 and the L4F mutant, currents were elicited using 1-s test pulses, whereas 2-s test pulses were used to elicit current families from the L1F, L2F, L3F, and L5F mutant channels. Time constants of inactivation (τ) were lengthened in all channel mutants (note: different time scale for hKv1.4 and L4F) and were determined by exponential fit of the decay of outward K^+ current. Current decay in hKv1.4 (τ = 25.92 ms), L2F (τ = 246.59 ms), and L5F (τ = 262.98 ms) was fit by a single exponential. However, current decay in L1F (τ_{fast} = 36.17 ms; τ_{slow} = 345.35 ms), L3F (τ_{fast} = 34.11 ms; τ_{slow} = 167.04 ms) and L4F (τ_{fast} = 50.41 ms; τ_{slow} = 209.97 ms) was fit by two exponentials.

mV; $n = 7$), and a 30-mV shift in L5F ($V_{1/2} = 18.34 \pm 1.91$ mV; $n = 5$). Figure 3A displays this pattern of 5- (L1F and L3F), 10- (L4F), 20- (L2F) and 30-mV (L5F) depolarizing shifts, showing a representative conductance-voltage relationship for each mutant channel construct. In addition, the most pronounced change was seen in the slope of the conductance-voltage curves of L5F, the slope factor being decreased to 7.60 (L5F) from 13.42 (hKvl.4).

Point mutations of the L2, L4, and L5 heptad leucines to Phe each produced a depolarizing shift in the voltage dependence of SS-inactivation that paralleled their respective activation shifts, whereas the L1F and L3F channels exhibited no change from that of the wild-type hKvl.4 channel. Representative SS-inactivation curves for each channel construct are shown in Fig. 3B and illustrate a pattern of depolarizing shifts that corresponds with the voltage dependent shifts in activation. The mean midpoint potentials ($V_{1/2}$) of the SS-inactivation curves in hKvl.4 ($V_{1/2} = -46.26 \pm 5.68$ mV; $n = 8$) resembled that in both L1F ($V_{1/2} = -45.45 \pm 3.13$ mV; $n = 2$) and L3F ($V_{1/2} = -47.74 \pm 0.40$ mV; $n = 2$). As with the voltage dependent changes in activation, the approximately 10 mV depolarizing shift in SS-inactivation in L4F ($V_{1/2} = -37.91 \pm 2.65$ mV; $n = 11$) was exceeded 2- to 3-fold in L2F ($V_{1/2} = -19.06 \pm 4.59$ mV; $n = 5$) and L5F ($V_{1/2} = -16.06 \pm 3.51$ mV; $n = 4$). There is some variation in the slope of the SS-inactivation curves for all constructs except L1F, with the greater changes occurring in L2F (increased) and L3F (decreased).

Effects of Heptad Leucine Mutations on 4-AP Sensitivity. Previously, we showed that the L4F mutation in hKvl.4 produced a dramatic 400-fold increase in steady-state block by 4-AP, even in the presence of the inactivation gate and that this change in 4-AP sensitivity was extant after removal of the inactivation gate (Judge et al., 1999). Here, we show that individual Phe-for-Leu substitutions for the other four heptad leucines in hKvl.4, which are not considered part of the 4-AP binding site, also increase channel sensitivity to block by 4-AP. Figure 4 shows the concentration-response curves for representative cells transfected with L1F, L2F, L3F, and L5F, compared with hKv1.4 and L4F. Like L4F, the L2F and L5F mutant channels each exhibited 400-fold increases in 4-AP sensitivity. The 4-AP half-blocking concentration (IC_{50}) in L2F was 1.49 ± 0.33 μM ($n = 3$) and 2.47 μM ($n = 1$) in L5F, compared with 1.88 ± 0.17 μM ($n = 4$) in L4F and 647.00 ± 29.00 μM ($n = 4$) in hKvl.4. The L1F and L3F mutations also increased 4-AP sensitivity but to lesser degrees: an 8-fold increase in sensitivity in L1F with an $IC_{50} = 82.86$ μM ($n = 1$), and a 150-fold increase in sensitivity L3F with an $IC_{50} = 4.60 \pm 1.50$ μM ($n = 2$). L4F exhibited the steepest concentration-response curve, with a Hill coefficient (n_H) of 2.36. For hKv1.4, L1F, L2F, L3F, and L5F, n_H is 1.33, 0.93, 0.78, 0.94, and 0.81, respectively. The pattern of increased 4-AP sensitivity in each of the heptad leucine mutant channels is similarly reflected in the differences in the ΔF of 4-AP in these channels (Fig. 5), with the mutant channels possessing the following order of ΔF for 4-AP: L2F $\approx$ L4F $\approx$ L5F $>$ L3F $>$ L1F.

Changes in 4-AP block were compared with changes in the channel gating properties of current deactivation and the voltage dependence of current activation and SS-inactivation. There is general association between altered channel gating and increases in 4-AP sensitivity after Phe-for-heptad-Leu substitutions in hKvl.4. In Fig. 6, the IC_{50} values for block by 4-AP are plotted against the deactivation time constants, elicited at test potentials of -60 mV (Fig. 6A) and -100 mV (Fig. 6B), for hKvl.4 and the five heptad leucine mutant channels. The solid lines represent first-order linear regression curve fits to all of the data points. Fitting all of the -60 mV data yielded a correlation coefficient (ρ) of 0.79 ($p > 0.05$), but removal of the L3F data point greatly improved the fit (dotted line) yielding a ρ value of 0.93 ($p < 0.01$). The fits to the -100 mV data, with L3F ($\rho = 0.82$; $p > 0.05$) and without L3F ($\rho = 0.89$; $p < 0.05$), showed a similar tendency. Thus, the channel constructs, L1F, L2F, L4F, L5F, and the wild-type hKv1.4, obey the empirical relationship, suggesting that the dramatic increases in 4-AP sensitivity are linked to changes in deactivation time constants. L3F does not obey this empirical relationship, indicating that other factors may be involved in determining the level of increased sensitivity to 4-AP in this mutant channel.

IC_{50} values of 4-AP to block K^+ channels were also compared with voltage dependence of activation and those of inactivation by plotting the IC_{50} for block by 4-AP against the midpoint potentials ($V_{1/2}$) of the conductance-voltage (Fig. 7A) and SS-inactivation relationships (Fig. 7B). There were no clear relationships between IC_{50} values and midpoints of activation (Fig. 7A) or inactivation (Fig. 7B). For examples, three mutants (L4F, L2F, and L5F) had similar IC_{50} values,

TABLE 1.
Deactivation kinetics for hKv1.4 and heptad leucine mutant channel constructs

Membrane Potential	τ_{tails} ($\pm$ SD_{n-1})					
	hKv1.4 ($n = 8$)	L1F ($n = 5$)	L2F ($n = 6$)	L3F ($n = 9$)	L4F ($n = 11$)	L5F ($n = 7$)
mV	*ms*					
−100	4.66 ± 1.19	2.38 ± 0.16	1.21 ± 0.83	2.72 ± 0.68	1.20 ± 0.46	2.26±1.18
−90	5.22 ± 1.26	2.77 ± 0.85	1.42 ± 0.89	3.17 ± 0.39	1.41 ± 0.62	2.08±0.67
−80	6.07 ± 2.15	3.13 ± 0.21	1.00 ± 0.50	3.61 ± 1.66	1.53 ± 0.44	3.20±2.64
−70	7.43 ± 1.84	3.42 ± 0.25	1.21 ± 0.47	5.55 ± 2.44	1.51 ± 0.54	2.73±1.82
−60	10.86 ± 2.57	3.68 ± 0.88	1.19 ± 0.62	6.06 ± 1.99	1.79 ± 0.58	2.75±1.42
−50	14.98 ± 6.29	2.81 ± 1.34[a]	1.40 ± 0.82	7.38 ± 1.81	1.68 ± 0.52[e]	1.96±0.88[b]
−40	11.37 ± 4.73[b]	4.08 ± 1.41[a]	1.72 ± 0.90	9.26 ± 1.68	2.36 ± 0.57[e]	3.14±1.68[c]
−30	6.62 ± 3.99[b]	5.40 ± 2.11[a]	1.30 ± 0.78	9.60 ± 3.52	2.31 ± 0.46[e]	2.78±2.00
−20	5.74 ± 2.64[b]	6.74 ± 2.88[a]	1.60 ± 0.70	7.87 ± 4.55[d]	2.31 ± 1.26[e]	2.30±0.54[a]

[a] $n = 4$.
[b] $n = 5$.
[c] $n = 6$.
[d] $n = 7$.
[e] $n = 8$.

yet they differed greatly in the midpoints of activation and inactivation.

It is known that the voltage dependence of inactivation derives mostly from the voltage dependence of activation. The correlation between voltage dependence of activation and 4-AP block was further analyzed by normalizing to their maximum depolarizing shifts (Fig. 7C). A linear regression

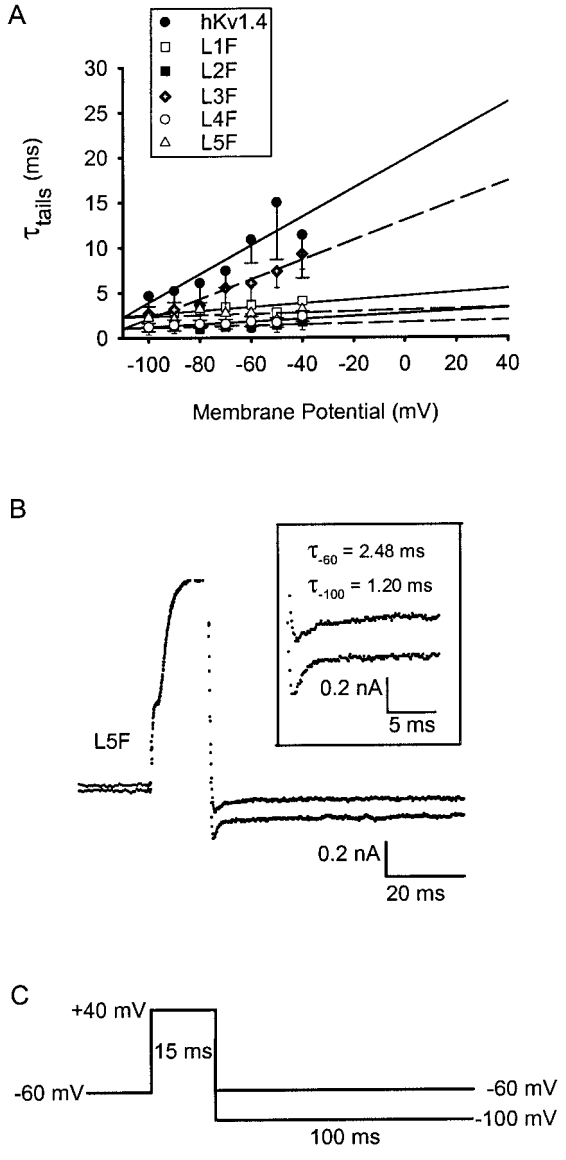

Fig. 2. Accelerated deactivation kinetics exhibit voltage dependence in hKv1.4 and L3F but not in L1F, L2F, L4F, and L5F. For deactivation kinetics, measured as the time constant of tail current decay, plotting the means from Table 1 (A) against the membrane potential at which the tail currents were elicited reveals comparable patterns of voltage dependent increases in tail current kinetics for hKv1.4 and L3F at voltages positive to −70 mV. First-order linear regression fits to the data reveal a strong correlation between increasing membrane depolarization and slowing tail current decay in L3F with a correlation coefficient (ρ) of 0.98 (A). In A, the mean ρ values for the other channel constructs are 0.89 (hKv1.4), 0.75 (L1F), 0.56 (L2F), 0.89 (L4F), and 0.30 (L5F). All linear regression fits were extrapolated to +40 mV. Tail currents were elicited by stepping from a holding potential of −60 mV to a single 15-ms prepulse of +40 mV and then stepping, for 300 ms, from −100 to 0 mV in 10-mV increments. Representative tail currents from L5F (B) are shown for the portion of the tail current protocol depicted in C. The B insert shows the L5F tail currents expanded and includes the deactivation time constants for the tail currents elicited at −60 and −100 mV.

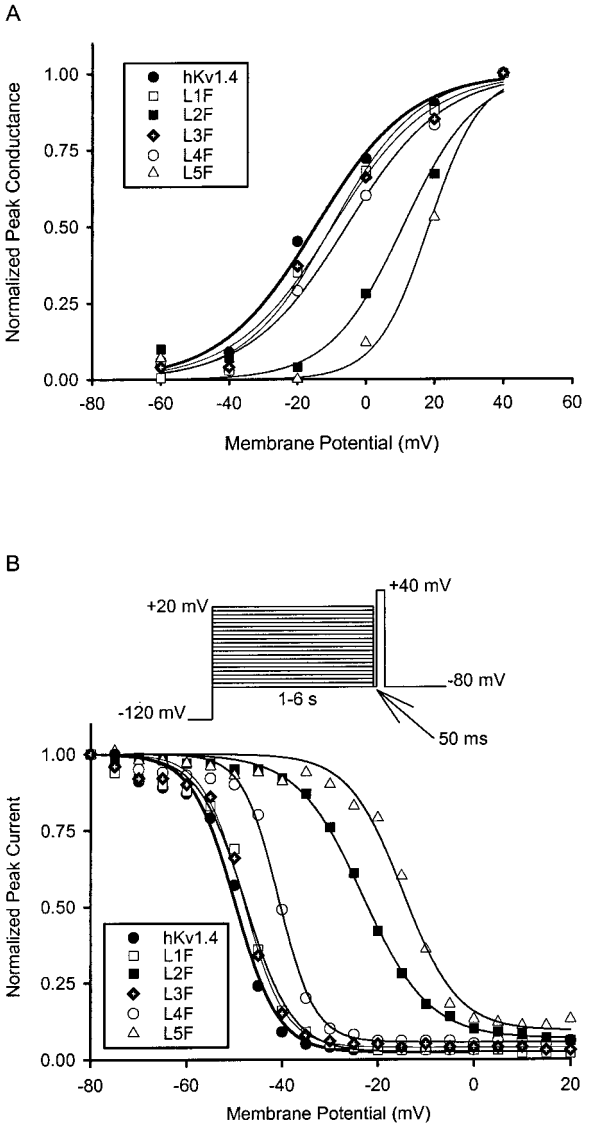

Fig. 3. Mutation of the heptad leucines to phenylalanine produces depolarizing shifts in both the voltage dependence of current activation (A) and steady-state inactivation (B) compared with hKv1.4. Shown in (A) and (B) are data from representative individual cells transfected with hKv1.4, L1F, L2F, L3F, L4F, and L5F. Representative conductance-voltage relationships (A) for peak outward conductance normalized to the maximal conductance of each channel illustrate the depolarizing shifts seen after individual phenylalanine substitutions for each heptad leucine. Compared with hKv1.4 ($V_{1/2}$ = −14.81 mV; k = 13.42), these depolarizing shifts are approximately 5 mV in L1F ($V_{1/2}$ = −9.93 mV; k = 12.79) and L3F ($V_{1/2}$ = −9.65 mV; k = 14.27), 10 mV in L4F ($V_{1/2}$ = −2.18 mV; k = 14.66), 20 mV in L2F ($V_{1/2}$ = 10.89 mV; k = 10.71), and 30 mV in L5F ($V_{1/2}$ = 18.38 mV; k = 7.60). Normalized data points are fit to the following Boltzmann equation: $g = 1/\{1 + \exp[-(V - V_{1/2})/k]\}$, where $V_{1/2}$ is the midpoint at which 50% of the K^+ channels are activated and k is the slope factor. Representative SS-inactivation curves (B) for peak outward current normalized to the maximal current after 1 sec (hKv1.4), and 2- or 6-s (mutant channels) prepulses illustrate the ~10 mV depolarizing shift seen in L4F ($V_{1/2}$ = −40.74 mV; k = 3.78; A = 0.06), and the 20- to 30-mV depolarizing shifts seen, respectively, in the L2F ($V_{1/2}$ = −23.08 mV; k = 6.87; A = 0.07) and L5F ($V_{1/2}$ = −14.72 mV; k = 5.71; A = 0.09) mutant channels. The L1F ($V_{1/2}$ = −47.66 mV; k = 4.92; A = 0.02) and L3F ($V_{1/2}$ = −47.45 mV; k = 2.76; A = 0.03) mutant channels exhibit voltage dependence of steady-state inactivation similar to the parent hKv1.4 ($V_{1/2}$ = −49.80 mV; k = 4.51; A = 0.02) channel. Normalized data points are fit to the following Boltzmann equation of the form: $h = (1 - A)/\{1 + \exp[(V_{1/2} - V)/k]\} + A$, where $V_{1/2}$ is the midpoint at which the availability of K^+ channels for activation is 50%, k is the slope factor, and A is the noninactivating component.

fit to all of the data points (dotted lines) still results in poorer correlation coefficients for activation ($\rho = 0.77$; $p > 0.05$). However, first-order linear regression fits to the data indicate that the strongest correlation exists between hKvl.4, L1F, L2F, and L5F (solid lines), where $\rho = 0.98$ ($p < 0.05$), while fitting the data points for hKvl.4, L1F, L3F and L4F (dashed lines) results in a insignificant correlation ($\rho = 0.90$; $p > 0.05$).

Discussion

In this study, we examined the role of phenylalanine (Phe) substitutions in the leucine heptad repeat region in determining channel gating and sensitivity to block by 4-AP in a cloned, rapidly inactivating human brain Kv1.4 K^+ channel. We were interested in Phe because it is the only amino acid other than leucine that is found naturally at the position of any of the heptad leucines exclusively present in the Kv3 (at L4) and the Kv4 (at L1) subfamilies of voltage-gated K^+ channels, which are known to exhibit enhanced sensitivity to 4-AP block. Here, in hKv1.4, we demonstrated that individual substitutions of Phe for each heptad Leu produce alterations in channel gating indicative of increased stabilization of the channel closed state that varies among the five heptad Leu mutant channels. Furthermore, we showed that these hKv1.4 mutations are accompanied by increases in the current blocking potency of 4-AP.

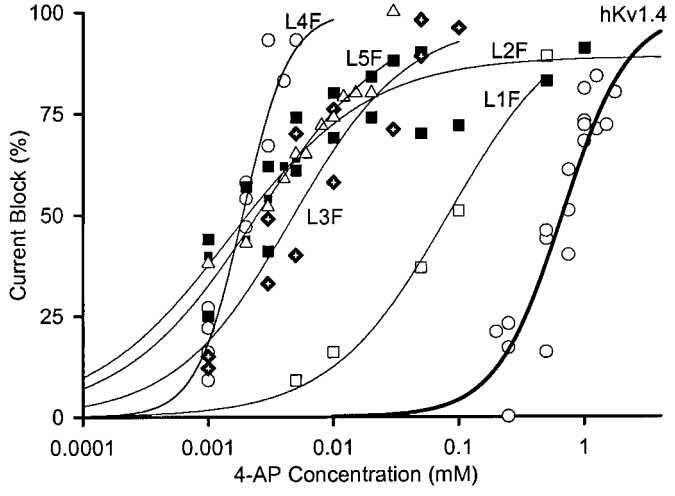

Fig. 4. Each of the individual phenylalanine for heptad leucine mutations increases channel sensitivity to block by 4-AP. Shown are the concentration-response curves for hKv1.4 (●), L1F (□), L2F (■), L3F (◆ with +), L4F (○), and L5F (△). Seen are ~400-fold increases in the sensitivity of 4-AP block in L2F [$IC_{50} = 1.49 \pm 0.33$ μM 4-AP ($n = 3$); $n_H = 0.78$], L4F [$IC_{50} = 1.88 \pm 0.17$ μM 4-AP ($n = 4$); $n_H = 2.36$], and L5F [$IC_{50} = 2.47$ μM 4-AP ($n = 1$); $n_H = 0.81$], a 150-fold increase in L3F [$IC_{50} = 4.60 \pm 1.50$ μM 4-AP ($n = 2$); $n_H = 0.94$] and an 8-fold increase in L1F [$IC_{50} = 82.86$ μM 4-AP ($n = 1$); $n_H = 0.93$] compared with hKv1.4 [$IC_{50} = 647.00 \pm 29$ μM 4-AP ($n = 4$); $n_H = 1.33$]. The normalized data points are fit to the following equation: $y = A \times x^{nH}/(x^{nH} + IC_{50}{}^{nH})$, where A = maximum current block and n_H = Hill coefficient. Each curve represents the fit to the mean for a given channel construct, or the fit to a single set of data points (L1F and L5F).

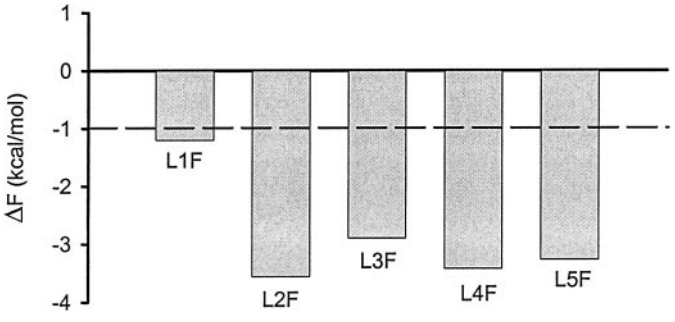

Fig. 5. The apparent free energy difference of binding (ΔF) for 4-AP in the five heptad leucine mutant channels shows moderate to strong increases in drug-channel interactions. Negative ΔF values indicate increased affinity for the binding of 4-AP in the mutant channels relative to hKv1.4. A moderate increase in 4-AP affinity was seen in L1F, where $\Delta F = -1.21$ kcal/mol. A stronger increase was seen in L3F, where $\Delta F = -2.90$ kcal/mol. The strongest increases in the relative free energy of binding were seen in L2F ($\Delta F = -3.56$ kcal/mol), L4F ($\Delta F = -3.42$ kcal/mol), and L5F ($\Delta F = -3.26$ kcal/mol). Measurements of the apparent free energy of binding were calculated as $\Delta F = RT \ln$ (IC_{50} of mutant channel/IC_{50} of parent hKv1.4 channel), where $R = 1.987$ cal/mol and $T = 295$°K.

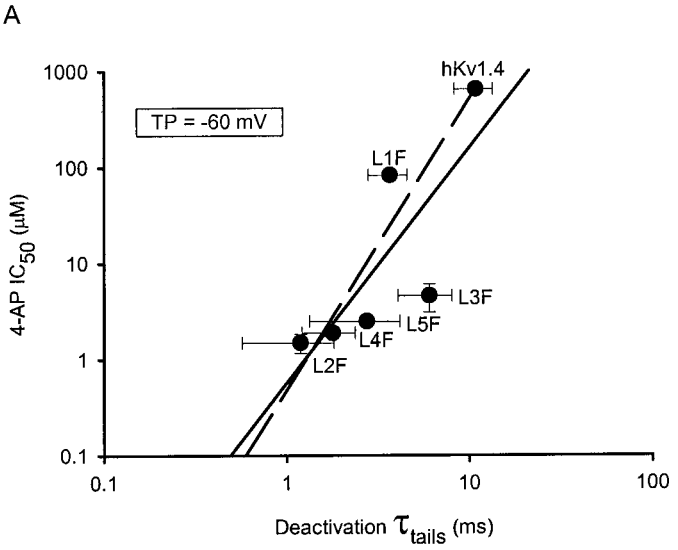

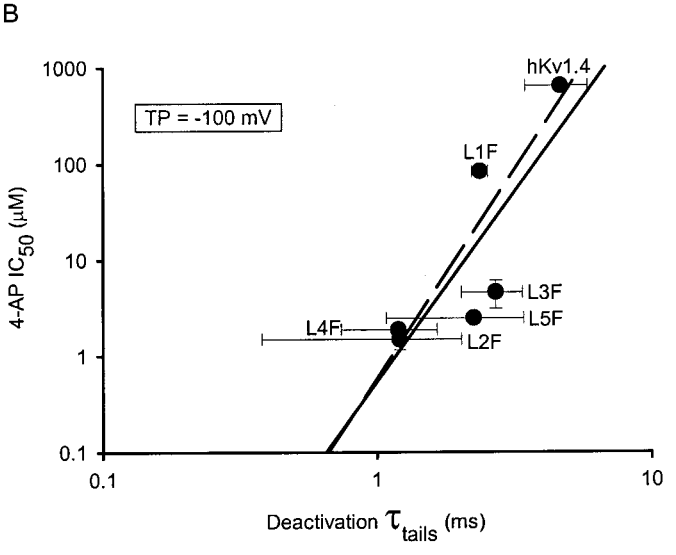

Fig. 6. Faster deactivation kinetics correlate best with increased 4-AP sensitivity in L2F and L4F. Shown are the mean IC_{50} values for 4-AP current block in hKv1.4 and the five heptad leucine mutant channels plotted against the mean deactivation kinetics for tail currents elicited at test potentials of −60 mV (A) and −100 mV (B), in each channel. First-order linear regression fits to all data points (solid lines) reveal $\rho = 0.79$ (A) and $\rho = 0.82$ (B). $\rho = 0.93$ (A) and $\rho = 0.89$ (B) for fits restricted to the hKv1.4, L1F, L2F, L4F and L5F data points (dashed lines).

From site-directed mutagenesis studies, it has been concluded that higher 4-AP sensitivity is associated with channel depolarizing shifts in current activation (McCormack et al., 1994; V1F and V2F mutations in *Shaker*), and with faster tail currents (Shieh and Kirsch, 1994; an L4F mutation in Kv2.1). In the present study, we found that magnitudes of parallel depolarizing shifts in the voltage dependence of current activation correspond to the levels of increased 4-AP sensitivity in the L1F, L2F, and L5F mutant channels (Fig. 7C) and that the extent of increased rates of current deactivation correspond to the levels of increased 4-AP sensitivity in the L1F, L2F, L4F and L5F mutant channels (Fig. 6). The only difference between these two relationships is that whereas L4F has a moderate shift in activation, it has the same increased 4-AP sensitivity as L2F and L5F mutations that exhibit greater depolarizing shifts in activation. Because L4F, L2F, and L5F have similar deactivation kinetics, the 400-fold increases in 4-AP sensitivity observed in these three mutant channels may be entirely accounted for by altered channel gating.

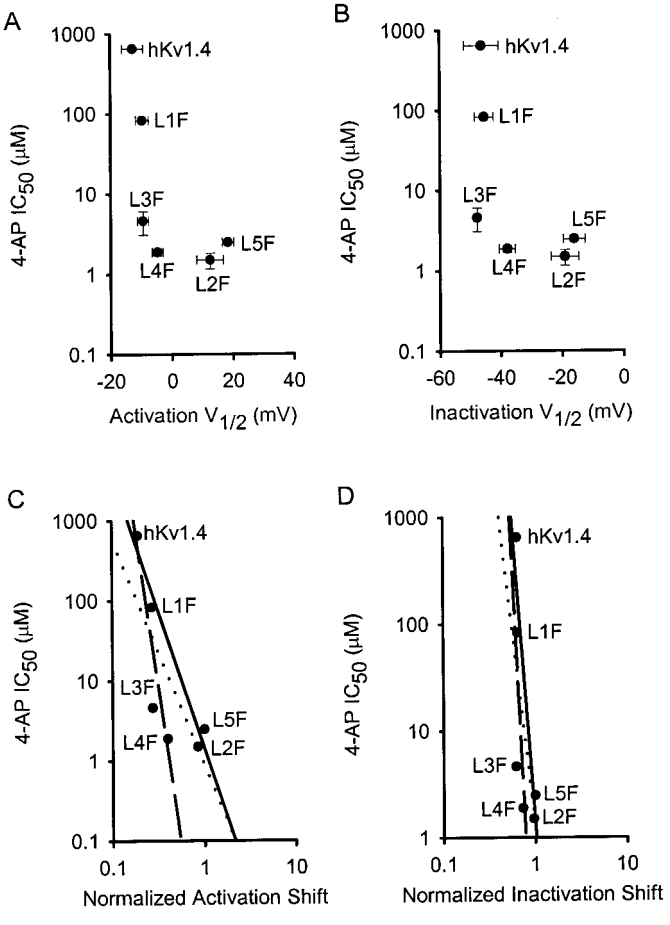

Fig. 7. Voltage dependent shifts, in the depolarizing direction, for current activation and SS-inactivation correlate best with increased 4-AP sensitivity in L1F, L2F, and L5F. Shown, for each channel construct, are the mean 4-AP IC_{50} values plotted against the mean midpoint potentials ($V_{1/2}$) for current activation (A) and SS-inactivation (B). Mean 4-AP IC_{50} values are plotted against $V_{1/2}$ values normalized to their maximal depolarizing shifts for current activation (C) and SS-inactivation (D). Correlation coefficients are determined for three different combinations of data points in both (C) and (D). For linear regression fits to hKv1.4, L1F, L2F, and L5F (solid lines), $\rho = 0.98$ for activation and 0.96 for inactivation. For hKv1.4, L1F, L3F, and L4F (dashed lines), $\rho = 0.90$ for activation and 0.52 for inactivation. For all data points (dotted lines), $\rho = 0.77$ for activation and 0.64 for inactivation.

The L327F (corresponding to our L478F:L4F) point mutation that increased 4-AP sensitivity 29-fold in a rat brain Kv2.1 K^+ channel (Shieh and Kirsch, 1994) was not accompanied by an acceleration of the rate of current deactivation. This result led them to conclude that L4F might be critical for 4-AP binding. In hKv1.4, however, the same L4F mutation produced a 400-fold increase in 4-AP sensitivity that was accompanied by faster deactivation kinetics, suggesting that our dramatic change is predominantly the result of altered channel gating. This notion is consistent with the singularly steep concentration-response relationship for 4-AP to block L4F (Fig. 4).

McCormack et al. (1991) demonstrated previously that *Shaker* K^+ channel subunit assembly did not depend on the leucine heptad repeat region, indicating that K^+ channel intersubunit interactions do not involve the classic coiled-coil interactions known as the leucine-zipper. Instead, they suggested that the heptad leucines are involved in converting charge movement into channel conformational changes. Our results are consistent with this conclusion that K^+ channel heptad leucines underlie voltage-dependent changes involved in the structural organization of K^+ channels related to gating.

Recent theoretical three-dimensional models of *Shaker* (Liu et al., 1997; Holmgren et al., 1998) and the Kvl family of voltage-gated K^+ channels (H. R. Guy, personal communication) show that the inner half of the ion translocation pathway is lined by the N-terminal end of the S6 segments, whereas the two ion-selective P segments form only the outer half of the K^+ channel pore (Durell et al., 1998). The current state of this model (H. R. Guy, personal communication) predicts that, within any given subunit of the channel homotetramer, gating-induced alterations in the environments of each heptad leucine result in changed intrasubunit interactions among the heptad leucines and with other residues (in S4–S5, S5, and S6) between the open and closed state. In particular, this model predicts intrasubunit heptad leucine interactions between L2 (S4–S5 linker) and L5 (N-terminal end of the S5 segment), as well as between L3 (S4–S5 linker) and L4 (N-terminal end of the S5 segment) in the open state, but only between L3 and L4 in the closed state. Based on this model, it is likely that the intrasubunit packing of L2, L3, L4, and L5 is energetically favorable for the open state and that the Phe-for-heptad-leucine substitutions destabilize the open conformation, thereby producing the observed shifts in the conductance-voltage curves for the mutant channels. Additional mutagenesis studies are underway to examine how individual substitution of the hKv1.4 heptad leucines with other amino acids will affect channel gating, as seen with valine for heptad Leu substitutions in *Shaker* (McCormack et al., 1991), and whether construction of a wild-type mutant channel dimer produces a functional channel phenotype exhibiting intermediate voltage-dependent and 4-AP sensitivity properties. Substantiating a direct role for the leucine heptad repeat region on channel properties requires a comprehensive evaluation of the effects of amino acid polarity and size and putative complementary amino acids, which interact with the heptad leucines, on channel gating. One approach to testing model-predicted residue proximities and interactions in our hKv1.4 heptad leucine mutant channels

would be to introduce suitable single and double cysteine substitutions for disulfide trapping of these channels in open or closed state conformations, as was done to test structural models for the gating mechanism in the large mechanosensitive MscL channel (Sukharev et al., 2001a,b).

Based on gating current experiments in the *Shaker* K^+ channel and mutant *Shaker* channels designed to isolate the final opening transitions in the gating process and to study the effects of 4-AP on channel activation (Loboda and Armstrong, 2001), Armstrong and Loboda (2001) propose a model for the action of 4-AP in K^+ channels in which 4-AP exerts its current blocking action by promoting closure of the activation gate once gaining access to the open channel. This model suggests that, despite only a minor acceleration of deactivation kinetics in the L3F mutant channel, the concurrence of increased stabilization of the channel closed state after 4-AP binding could enhance 4-AP sensitivity. If this interpretation of our data in light of the current Armstrong and Loboda model is correct, we predict that K^+ currents in noninactivating variants of our mutant heptad L3F channels will show a time-dependent block by 4-AP and that the activation gating rate constants for 4-AP–bound channel transition from gate-open to gate-closed conformation, determining the deactivation kinetics (Armstrong and Loboda, 2001) necessary to simulate these gating currents, will be predictably larger in the heptad leucine mutants than in the wild-type hKv1.4.

Acknowledgments

We thank both Dr. H. Robert Guy and Dr. Kunihiko Goto for helpful discussions. In particular, we are grateful to Dr. H. Robert Guy for a critical reading of the manuscript. We are indebted to Yvonne M. Logan for her superior handling of the tissue culture and transfection requirements for this research.

References

Aggarwal SK and MacKinnon R (1996) Contribution of the S4 segment to gating charge in the Shaker K^+ channel. Neuron **16:**1169–1177.

Armstrong CM and Loboda A (2001) A model for 4-aminopyridine action on K channels: Similarities to tetraethylammonium ion action. *Biophys J* **81:**895–904.

Durell SR, Hao Y, and Guy HR (1998) Structural models of the transmembrane region of voltage- gated and other K^+ channels in open, closed, and inactivated conformations. *J Struc Biol* **121:**263–284.

Holmgren M, Shin KS, and Yellen G (1998) The activation gate of a voltage-gated K^+ channel can be trapped in the open state by an intersubunit metal bridge. *Neuron* **21:**617–621.

Janicki S and Monteiro MJ (1997) Increased apoptosis arising from increased expression of the Alzheimer's disease-associated presenilin-2 mutation. *J Cell Biol* **139:**485–495.

Judge SIV, Monteiro MJ, Yeh JZ, and Bever CT (1999) Inactivation gating and 4-AP sensitivity in human brain Kvl.4 potassium channel. *Brain Res* **831:**43–54.

Kirsch GE and Drewe JA (1993) Gating-dependent mechanism of 4-aminopyridine block of two related potassium channels. *J Gen Physiol* **102:**797–816.

Kirsch GE, Shieh C-C, Drewe JA, Verner DF, and Brown AM (1993) Segmental exchanges define 4-aminopyridine binding and the inner mouth of K^+ pores. *Neuron* **11:**503–512.

Liu Y, Holmgren M, Jurman ME, and Yellen G (1997) Gated access to the pore of a voltage-dependent K^+ channel. *Neuron* **19:**175–184.

Loboda A and Armstrong CM (2001) Resolving the gating charge movement associated with late transitions in K channel activation. *Biophys J* **81:**905–916.

Lopez GA, Jan YN, and Jan LY (1991) Hydrophobic substitution mutations in the S4 sequence alter voltage-dependent gating in Shaker K^+ channels. *Neuron* **7:**327–336.

McCormack K, Campanelli JT, Ramaswami M, Matthew MK, and Tanouye MA (1989) Leucine-zipper motif update. *Nature (Lond)* **340:**340.

McCormack K, Joiner WJ, and Heinemann SH (1994) A characterization of the activating structural rearrangements in voltage-dependent *Shaker* K^+ channels. *Neuron* **12:**301–315.

McCormack K, Tanouye MA, Iverson LE, Lin J-W, Ramaswami M, McCormack T, Campanelli JT, Mathew MK, and Rudy B (1991) A role for hydrophobic residues in the voltage-dependent gating of Shaker K^+ channels. *Proc Natl Acad Sci* USA **88:**2931–2935.

Pennington MW, Mahir VM, Khaytin I, Zaydenberg I, Byrnes ME, and Kem WR (1996) An essential binding surface for ShK toxin interaction with rat brain potassium channels. *Biochem* **35:**16407–16411.

Rauer H, Pennington M, Cahalan M, and Chandy KG (1999) Structural conservation of the pores of calcium-activated and voltage-gated potassium channels determined by a sea anemone toxin. *J Biol Chem* **274:**21885–21892.

Shieh C-C and Kirsch GE (1994) Mutational analysis of ion conduction and drug binding sites in the inner mouth of voltage-gated K^+ channels. *Biophys J* **67:**2316–2325.

Shieh C-C, Klemic KG, and Kirsch GE (1997) Role of transmembrane segment S5 on gating of voltage-dependent K^+ channels. *J Gen Physiol* **109:**767–778.

Sukharev S, Betanzos M, Chiang C-S, and Guy HR (2001a) The gating mechanism of the large mechanosensitive channel MscL. *Nature (Lond)* **409:**720–724.

Sukharev S, Durell SR, and Guy HR (2001b) Structural models of the MscL gating mechanism. *Biophys J* **81:**917–936.

Address correspondence to: Susan I. V. Judge, Ph.D. Department of Neurology, University of Maryland School of Medicine, BRB 12–040, 655 West Baltimore Street, Baltimore, MD 21201. E-mail: sjudge@umaryland.edu